

# An Optimal Sensor Management Technique for Unmanned Aerial Vehicles Tracking Multiple Mobile Ground Targets

Negar Farmani<sup>1</sup>, Liang Sun, Daniel Pack

**Abstract**—In this paper, we present an optimal sensor management technique for an Unmanned Aerial Vehicle (UAV) to autonomously geo-localize multiple mobile ground targets. The target states are continuously estimated using target locations asynchronously captured by a gimbaled camera with a limited field of view and processed with a set of Extended Kalman Filters (EKF). The technique incorporates a Dynamic Weighted Graph (DWG) method to first group estimated targets and then determine regions with high target densities. A Model Predictive Control (MPC) method is used to compute a camera pose that minimizes the overall uncertainty of the target state estimates. The validity of the proposed technique is demonstrated using simulation results.

## I. INTRODUCTION

Over the past two decades, we have witnessed the increasing number of applications of UAVs, with corresponding research interests in the UAV community. The UAV applications include missions for both civilian and military operations such as search and rescue, ocean exploration, border security, natural disaster assessment, and a variety of military missions. One of the key capabilities of any UAV is its ability to search, detect, and locate ground targets. In particular, for future UAV applications such as ones that will be performed by the law enforcement, autonomous tracking of mobile targets is a critical capability of a UAV. Although, as we will show, researchers have studied the target tracking problem and reported feasible solutions, there is lack of techniques to track multiple targets in some optimal manner when the resources (sensors) are limited to fully carry out the mission. To track ground targets, different onboard sensors such as electro-optic and infrared cameras have been used in the past. The electro-optic camera is widely used due to its compact nature, cost, and existing software for image exploitation. The limitations of the resolution, the range, and the field of view (FOV) of a camera, however, introduce new challenges. This paper presents an optimal technique to optimally manage a single sensor resource, a gimbaled camera with a limited field of view, to track multiple mobile ground targets.

Several methods were proposed to address the problem of target tracking and geo-location using UAVs. Redding et al. [1] reported a method for a UAV to geo-locate a target using a Recursive Least Square filter. However, this method is only suitable for stationary targets. Theodorakopoulos and Lacroix [2] presented a control strategy based on a A\*

method for a UAV to track a ground target by optimizing the target visibility likelihood derived from a position history of the target. Li et al [3] reported a target tracking method using a camera and motion estimates of a ground target to control a UAV such that it maintains a fixed horizontal distance from the target. For target motion estimation, they applied a fast adaptive estimator and L1 adaptive control law for the gimbaled camera to keep the target in the center of the image frame. Han and DeSouza [4] presented a method for a UAV to geo-localize and track multiple-targets using an airborne video camera. They used optic flow and a SIFT (Scale Invariant Feature Transformation) based algorithm to track multiple targets. It was shown that the multi-stereo technique which uses image sequences increased the accuracy of the target geo-location. Grocholsky et al. [5] reported a recursive filter that improved geo-location estimates of targets by handling large, time-varying and non-Gaussian sensor errors. Tisdale et al. [6] proposed a method for multiple UAVs to search for a target using a combined probabilistic search and tracking technique based on a particle filter. Although the paper showed promising results, the computation cost would be high for real-time implementation. Morbidi et al. [7] proposed a gradient-based control strategy and used a Kalman Filter to estimate target positions using a team of aerial vehicles. Mousumi et al. [8] used an EKF for a vision based state estimator and target tracking using multiple UAVs by incorporating a 3D nonlinear guidance controller. They used a directed graph to represent the cooperation among vehicles. Sharma and Pack [9] developed a technique to geo-localize multiple ground targets using a team of UAVs. Cooperative estimation of target positions were computed using a data fusion technique.

In this paper, we focus on capabilities of a single UAV with a gimbaled camera with a limited FOV tracking multiple mobile targets, which was not done in previous works reported. We propose a novel technique that extends the work in [9] by first generating candidates for a gimbal pose based on a dynamic weighted graph, incorporating density information of observable multiple targets, to evaluate possible gimbal poses and determine an optimal gimbal configuration that minimizes the overall target position uncertainties (the sum of all target positions in covariance matrices) using a Model Predictive Control (MPC) method. In [9], the gimbal pointing decision was done based on a single target uncertainty rather than considering the location density of multiple targets. As for the UAV path generation, it was updated in [9] to move toward a target with the largest uncertainty, but in the current proposed work, the path of a UAV is generated based on

<sup>1</sup> Authors are with the Department of Electrical and Computer Engineering, University of Texas at San Antonio. fkv344@my.utsa.edu, liang.sun@utsa.edu, daniel.pack@utsa.edu

again multiple targets rather than a single target, reducing the need to rapidly change path directions of a UAV and the pose of an onboard gimbal.

The rest of the paper is arranged as follows. In Section II, we describe the problem we propose to solve and presents the technique we developed. Section III offers the analysis of simulation results for a single UAV tracking multiple targets and, finally, we conclude the paper with some future research directions identified in Section IV.

## II. PROBLEM STATEMENTS AND SENSOR MANAGEMENT

Consider a UAV with a gimballed camera tracking multiple targets moving on a flat ground. A gimballed camera with sensor noise captures images of targets, which are processed to estimate positions and velocities of targets. We assume that target movements are random sequences of piece-wise linear segments moving with velocities smaller than the one of the UAV, the UAV flies at a constant altitude and velocity, and the control input for the UAV is its bank angle. We also assume that the camera's field of view (FOV) is limited and the captured target status can be estimated with a Gaussian probability density function.

Given the above assumptions, the problem we seek to solve is the minimization of overall uncertainty of target locations over time by two control factors: position of the UAV and the pose of the onboard gimballed camera. We show in the next section the process we use to capture and locate targets and the underlying principles of the proposed technique to derive the gimballed camera pose and the path of a UAV.

Before presenting the proposed technique, we briefly describe the problem associated coordinate frames and the camera image projection method we used in the proposed technique. We then present the process used to estimate the location of each target followed by the proposed technique that uses a dynamic weighted graph (DWG) and an MPC based optimization strategy to determine an optimal direction for gimbal pointing. The UAV path is updated to direct the UAV toward the direction pointed by the gimballed camera.

### A. Camera and Gimbal Frames and Target Projection

Consider a UAV tracking  $n$  mobile targets. The position of the UAV in the North, East and Down (NED) inertial coordinate frame is represented by  $\mathbf{p}_u^i = [p_n^i, p_e^i, p_d^i]^T$ . The position of the  $k^{th}$  target in the same inertial frame is given by  $\mathbf{p}_k^i = [p_{kn}^i, p_{ke}^i, 0]^T$  where the superscript  $i$  represents an inertial frame. We assume that the origins of gimbal and camera frames are located at the center of mass of the UAV. There are three frames of interest: the body frame  $F_b \triangleq (i^b, j^b, k^b)$ , the gimbal frame  $F_g \triangleq (i^g, j^g, k^g)$  and the camera frame  $F_c \triangleq (i^c, j^c, k^c)$ , as shown in Fig. 1 and Fig. 2. The  $F_v \triangleq (i^v, j^v, k^v)$  is the vehicle frame with the origin at the center of mass of the UAV with its axes aligned with the axes of the inertial frame. The rotation matrix that relates

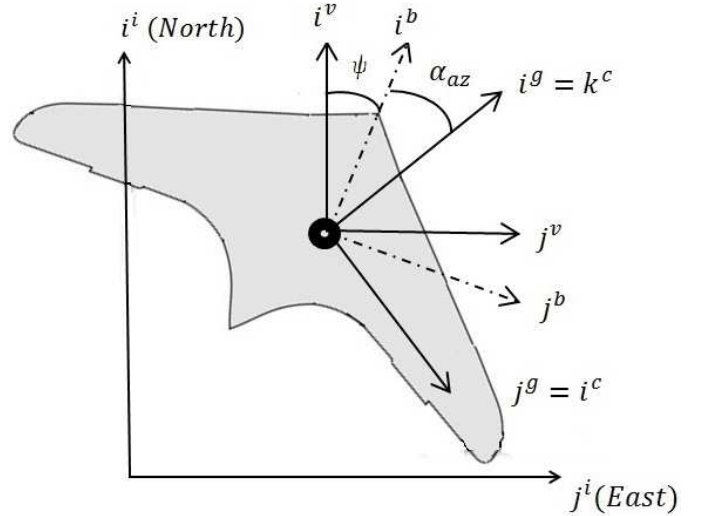


Fig. 1. Top view depicting the relationships among the gimbal, camera, body and vehicle frames

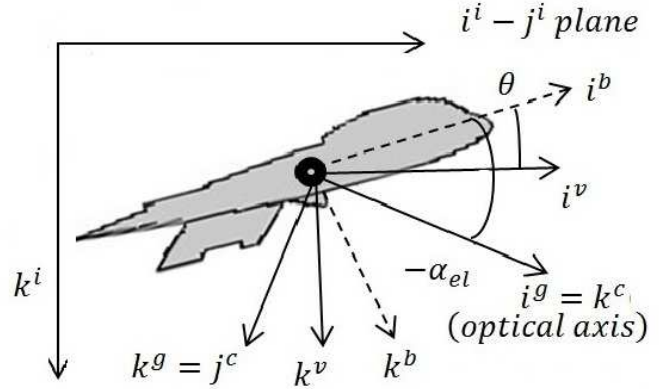


Fig. 2. Side view depicting the relationships among the gimbal, camera, body and vehicle frames

the body frame with the gimbal frame is given as [11]

$$R_b^g \triangleq \begin{pmatrix} \cos \alpha_{el} \cos \alpha_{az} & \cos \alpha_{el} \sin \alpha_{az} & -\sin \alpha_{el} \\ -\sin \alpha_{az} & \cos \alpha_{az} & 0 \\ \sin \alpha_{el} \cos \alpha_{az} & \sin \alpha_{el} \sin \alpha_{az} & \cos \alpha_{el} \end{pmatrix}, \quad (1)$$

where  $\alpha_{az}$  and  $\alpha_{el}$  are the azimuth and elevation angles of the gimbal with respect to the UAV body frame. The transformation (rotational matrix) from the gimbal frame to the camera frame is represented as

$$R_g^c \triangleq \begin{pmatrix} 0 & 1 & 0 \\ 0 & 0 & 1 \\ 1 & 0 & 0 \end{pmatrix}. \quad (2)$$

A target is projected into the camera frame and translated to a specific pixel location,  $\epsilon_x$  and  $\epsilon_y$  (in units of pixels), in the image plane. The gimballed camera pointing direction is determined by aligning the optical axis of the camera to the desired direction. As shown in Fig. 3, we define  $\tilde{l}^c$  as the desired direction of optical axis in the camera frame, which

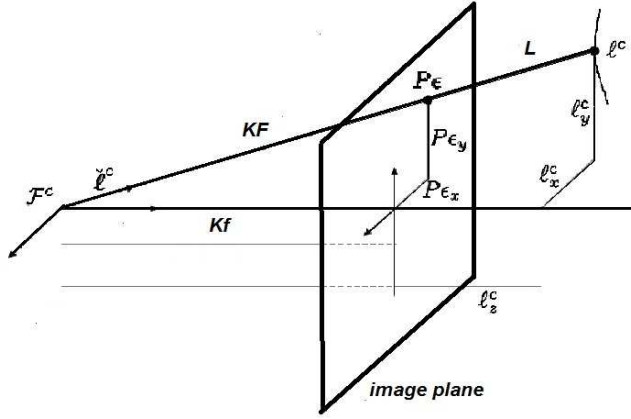


Fig. 3. The camera frame. Target in the camera frame is represented by  $\check{l}^c$  [11]

can be calculated by

$$\check{l}^c = \frac{1}{L} = \frac{1}{F} \begin{pmatrix} \varepsilon_x \\ \varepsilon_y \\ f \end{pmatrix}, \quad (3)$$

where  $f$  is the focal length of the camera and  $L = \|\mathbf{l}\| = \|\mathbf{p}_k - \mathbf{p}_u\|$  and  $F$  is

$$F \triangleq \sqrt{\varepsilon_x^2 + \varepsilon_y^2 + f^2}. \quad (4)$$

The desired direction of the optical axis in the body frame is

$$\check{l}_d^b = R_g^b R_c^g \check{l}^c, \quad (5)$$

and the pan-tilt gimbal motion equations are given by

$$\begin{aligned} \dot{\alpha}_{az} &= u_{az} \\ \dot{\alpha}_{el} &= u_{el}, \end{aligned} \quad (6)$$

where  $u_{az}$  and  $u_{el}$  are control inputs for the gimbal's azimuth and elevation angles, respectively.

In the camera frame the optical axis is given by  $(0,0,1)^T$ . In order to determine the commanded gimbal angles  $\alpha_{az}^c$  and  $\alpha_{el}^c$  that will align the optical axis with  $\check{l}_d^b$ , we need to solve  $\alpha_{az}^c$  and  $\alpha_{el}^c$  from the following equation.

$$\check{l}_d^b = \begin{pmatrix} \check{l}_{xd}^b \\ \check{l}_{yd}^b \\ \check{l}_{zd}^b \end{pmatrix} = R_g^b(\alpha_{az}^c, \alpha_{el}^c) R_c^g(0,0,1)^T. \quad (7)$$

The desired command angles are

$$\begin{aligned} \alpha_{az}^c &= \tan^{-1} \left( \frac{\check{l}_{yd}^b}{\check{l}_{xd}^b} \right) \\ \alpha_{el}^c &= \sin^{-1}(\check{l}_{zd}^b). \end{aligned} \quad (8)$$

The gimbal servo command is selected as

$$\begin{aligned} u_{az} &= k_{az}(\alpha_{az}^c - \alpha_{az}) \\ u_{el} &= k_{el}(\alpha_{el}^c - \alpha_{el}), \end{aligned} \quad (9)$$

where  $k_{az}$  and  $k_{el}$  are control gains based on the current error values [11].

## B. Geo-localization

To estimate positions and velocities of ground mobile targets, we use a set of EKFs. We assume that a UAV measures its pose in a world coordinate frame using a Global Positioning System (GPS) signals and Inertial Measurement Unit (IMU). Performing the coordinate transformations, the position of the target  $k$  becomes

$$\mathbf{p}_k^i = \mathbf{p}_u^i + R_b^i R_g^b R_c^g \check{l}_k^c, \quad (10)$$

where  $\check{l}_k^c$  is the normal vector of target  $k$  with respect to the camera frame and

$$R_b^i \triangleq \begin{pmatrix} c_\theta c_\psi & c_\theta s_\psi & -s_\theta \\ s_\phi s_\theta c_\psi - c_\phi s_\psi & s_\phi s_\theta s_\psi + c_\phi c_\psi & s_\phi c_\theta \\ c_\phi s_\theta c_\psi + s_\phi s_\psi & c_\phi s_\theta s_\psi - s_\phi c_\psi & c_\phi c_\theta \end{pmatrix}, \quad (11)$$

$c_\theta \triangleq \cos(\theta)$  and  $s_\theta \triangleq \sin(\theta)$ . The angles  $\phi, \theta, \psi$  are roll, pitch and yaw angles of the UAV, respectively.

Assuming that UAV is flying at a constant airspeed and wind speed is zero, the dynamics of the UAV is given by

$$\begin{pmatrix} \dot{p}_n \\ \dot{p}_e \\ \dot{h} \end{pmatrix} = V_a \begin{pmatrix} \cos \psi \\ \sin \psi \\ 0 \end{pmatrix} \quad (12)$$

where  $V_a$  is the UAV airspeed. The coordinated turn condition in terms of heading angle ( $\psi$ ) and constant airspeed is given by

$$\psi = \frac{g \tan \phi}{V_a}, \quad (13)$$

where

$$\dot{\phi} = k_\phi(\phi^c - \phi_i), \quad (14)$$

$g$  is the gravitational acceleration,  $k_\phi$  is a positive constant and

$$\phi^c = \tan^{-1} \left( \frac{p_{ke} - p_{ue}}{p_{kn} - p_{un}} \right). \quad (15)$$

The motion model for the  $i^{th}$  target is

$$\dot{x}_i = y_i(x_i, u) + Q. \quad (16)$$

The state for each target is define  $x_i = [x_{ni}, x_{ei}, v_{ni}, v_{ei}, L_i]^T$ , where  $x_{ni}$ ,  $x_{ei}$ ,  $v_{ni}$  and  $v_{ei}$  are the  $i^{th}$  target's position and velocity in the north and east directions, respectively.  $L_i$  is the range between the  $i^{th}$  target and the UAV and  $y_i = (v_{ni}, v_{ei}, 0, 0, L_i)^T$ .  $Q$  is the motion model Gaussian noise. For each target  $x_i$ , the prediction step of the EKF in discrete time is given by

$$\begin{aligned} \hat{x}_k &= \hat{x}_{k-1} + T_s y_i(\hat{x}_{k-1}, u_k) \\ P_k^- &= P_{k-1}^+ + T_s(A_{k-1}P_{k-1}^+ + P_{k-1}^+ A_{k-1}^T + Q) \end{aligned} \quad (17)$$

where  $\hat{x}$  is the estimated value of the state  $x$ ,  $A = \frac{\partial y}{\partial x}(\hat{x}, u)$  is the system Jacobian matrix,  $P$  is the state covariance matrix,  $T_s$  is the sampling period and  $+, -$  superscripts represent after and before measurement updates. The measurement model for the  $i^{th}$  target is  $h_i(x) = p_i - L_i R_b^i R_g^b R_c^g \check{l}_d^c$ . The measurement update of EKF is given by

$$\begin{aligned}
C_k &= P_k^- H_k^T (R + H_k P_k^- H_k^T)^{-1} \\
P_k &= (I - C_k H_k) \bar{P}_k^- \\
\hat{x}_k &= \hat{x}_k + C_k (z_k - h(\hat{x}_k, u_k)),
\end{aligned} \tag{18}$$

where  $H = \frac{\partial h_i}{\partial x} = [I \ R_b^i R_c^s \check{c}]$  is the measurement Jacobian matrix and  $C$  is the Kalman gain.

### C. Candidate Generation and Gimbal Pointing

To determine an optimal gimbal pointing direction for the purpose of minimizing the overall uncertainty of targets, a dynamic weighted graph (DWG) method is proposed. The DWG method generates gimbal pointing direction candidates for the Model Predictive Control (MPC) based optimization technique, which we will describe in this section.

For the DWG method, we define a graph  $G \triangleq [g_{ij}] \in \mathbb{R}^{n \times n}$  which represents connections among targets based on the distance between each pair with the connection value defined as

$$g_{ij} = \begin{cases} 0 & \text{if } i = j \\ \frac{e^{-|d_{ij}|}}{\sqrt{(\delta_{x_i} + \delta_{x_j})^2 + (\delta_{y_i} + \delta_{y_j})^2}} & \text{if } i \neq j \end{cases} \tag{19}$$

where  $d_{ij}$  represents the estimated distance between targets  $i$  and  $j$ ,  $\delta_{x_i}$ ,  $\delta_{x_j}$ ,  $\delta_{y_i}$  and  $\delta_{y_j}$  are estimated position variances of targets  $i$  and  $j$  in the north and east directions, respectively.

For two distinct targets  $i$  and  $j$ , the numerator of Equation (19) awards targets that are closer to each other. The denominator of Equation (19) incorporates the uncertainties of the position estimates for both the  $i^{th}$  and  $j^{th}$  targets. The bigger the uncertainties of the targets, the smaller the  $g_{ij}$  value, representing that we should weigh the numerator based on the amount of 'belief' we have for the position estimates.

The resulting matrix,  $G$ , is a symmetric matrix that shows the weighted distances among targets being estimated. The DWG is computed during each target estimation iteration to reflect the changing topology of targets. To find the possible gimbal pose candidates, we first sum each column (one can replace 'column' with 'row' in the subsequent discussion since  $G$  is symmetric) of matrix  $G$ . Note that the  $i^{th}$  column sum measures the estimated density of targets near target  $i$ . That is, the larger this value is, the more the targets are close to target  $i$ . By comparing the sums of columns, we rank order the densities of neighboring targets for each target. Using the density information, we then select top  $n$  column sums to generate camera gimbal pose candidates.

To develop a list of the candidates, we now bring the sensor constraints into consideration. In particular, we incorporate the camera's FOV and the UAV's ability to observe those targets. The sums of columns we obtained from matrix  $G$  give the locations of targets around which the high density of neighboring targets resides. To compute the merit of each camera gimbal pose, we first need to know whether or not the camera with its FOV can capture those targets. The answer to the question, however, depends on a pre-determined camera pose. To remedy this circular reasoning, we use the mean between the  $i^{th}$  target and its closest

neighbor as the camera gimbal pointing direction and apply the camera FOV constraints to determine the number of targets that can be captured. We acknowledge that there may be other solutions to this problem, which is one of the topics we will pursue in our future research.

Although the possible number of candidates for the optimal gimbal pose is the number of columns of matrix  $G$  in this set up, to reduce the computational complexity associated with selecting the candidates for our real-time control application of tracking mobile targets, we selected top three candidates for further evaluation using the below MPC method. The function is designed to minimize the current overall uncertainty of targets.

$$\min \prod_{i=1}^n \text{tr}(P_i^{-1} + a_i H^T R^{-1} H)^{-1} \tag{20}$$

$$\sum_{i=1}^{n_{FOV}} a_i = \text{number of targets in FOV},$$

where  $a_i \in \{0, 1\}$ .

Similar arguments as shown in Equation (20) are often found in Extended Information Filters (EIF) [10]. The motivation of using the expression in Equation (20) is that it succinctly captures the desired characteristics of both target uncertainties and our ability to capture targets using on-board sensors. An inverse of the state covariance matrix,  $P_i$ , known as the information matrix, represents our best current knowledge of target  $i$  and  $H^T R^{-1} H$  represents additional information, which describes the 'gains', the UAV will have if it chooses to capture target  $i$  using the onboard sensor with its sensor noise. By taking the inverse of the arguments in Equation (20), we obtain the combined covariance. The trace of the resulting matrix again captures overall variance of target  $i$ , incorporating sensor limits. The multiplication operator, in place of summation operator, is used to amplify the difference between gimbal pose candidates. Finding the minimum of the overall expression leads to the optimal gimbal pose (pointing direction). One final note on how UAV's trajectory is updated. For a single UAV, we simply use the ground location that matches the center of the selected sensor FOV as the new destination point for the UAV. This destination, as with the candidate selection, is updated each iteration cycle.

## III. EXPERIMENTAL RESULTS

In this section, we show the effectiveness of the technique proposed in the previous section using MATLAB/SIMULINK simulations. The primary emphasis of experiments is to compare the results of the current technique with the one we reported in [9]. The experiment consists of 100 runs of a single UAV, equipped with a gimballed camera with the limited FOV of 40 degrees, tracking five mobile targets in an urban environment. Each run lasts for 100 seconds and we assume that it takes two seconds each to change the pose of the gimbal camera, to process sensor information, to compute the next optimal gimbal pose, and to move the mechanical parts of the gimbal. Targets moved with a constant speed (5m/s) in a piece-wise linear fashion,

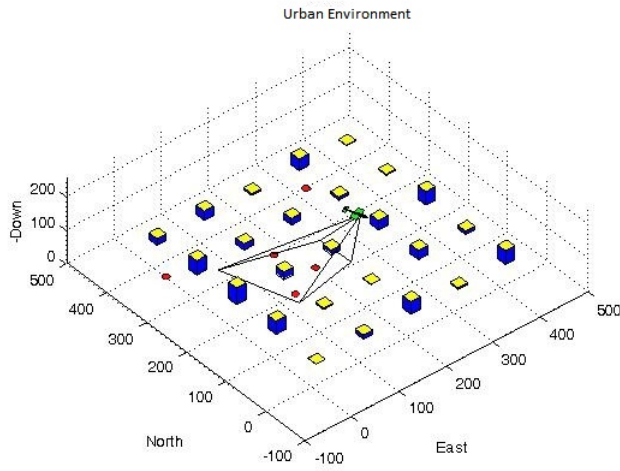


Fig. 4. Simulation environment

mimicking cars moving on city roads. Fig. 4 shows the environment within which the UAV operated and Fig. 5 shows the trajectories of targets. The speed of the UAV was constant at 13m/sec.

Fig. 6 through Fig. 10 show the results from a typical experimental run using both the proposed method and the method reported in [9]. The figure contains geo-location errors of five targets in the north and east directions, respectively. Results from the proposed method (solid line, DWG) and our previous algorithm (dashed lines, Sharma) are shown in each figure. All environmental conditions, including target motions were identical for both methods. It is clear from the figures that the error variations resulted from the proposed technique is smoother and smaller than the ones resulted from using the algorithm reported in [9]. The improvement of the proposed method is due to its ability to capture more than one targets whenever it is possible. The optimal gimbal pose chosen considering multiple targets also reduced the amount of initial ‘overshoot’ of error toward its desired zero value, when the results were compared with those generated by the previous method.

Table I shows the average errors of each target position estimation in the north and east directions, respectively, for the 100 experiments using both methods. Table II shows the overall position estimation errors of five targets in the north and east directions, respectively. It shows that the proposed method outperformed the one in [9] by 14% and 16% in the north and east directions, respectively.

Fig. 11 shows the statistics of the amount of time allocated by the UAV to capture each target. The y-axis represents the number of times the UAV chose a particular target to observe and the x-axis shows the target number. Target number six represents cases when more than a single target were captured by the UAV.

#### IV. CONCLUSION AND FUTURE WORKS

In this paper we proposed and demonstrated a new sensor management technique for UAVs tracking multiple targets.

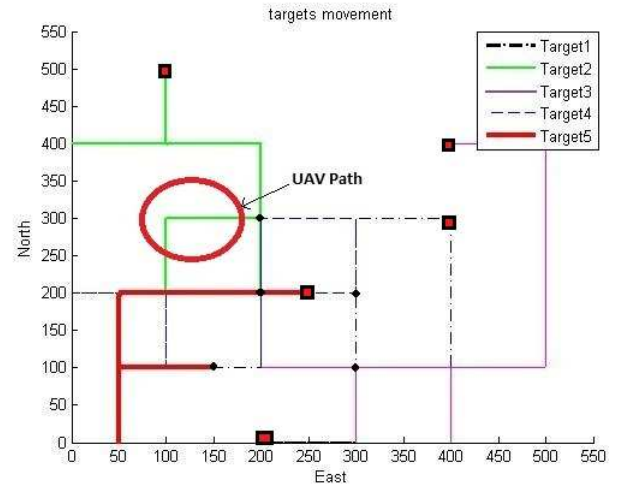


Fig. 5. The sample trajectories of five targets. The black dots show the start position and squares show the end position of each target movement.

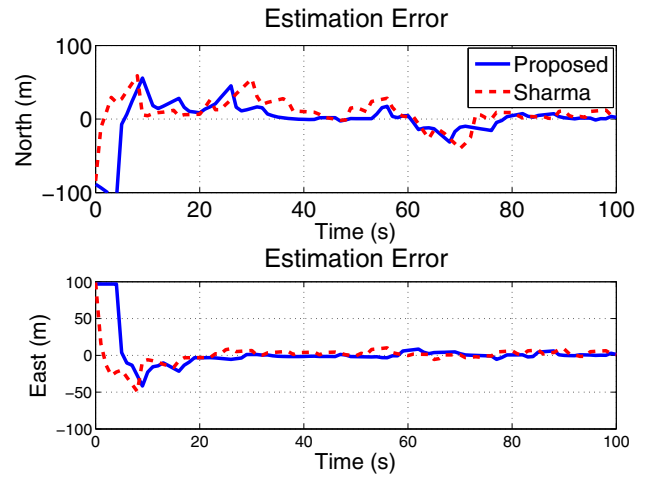


Fig. 6. Geo-location errors resulted from running the proposed method and the one reported in [9] for Target 1.

TABLE I  
AVERAGE GEO-LOCATION ERRORS OF FIVE TARGETS IN THE NORTH AND EAST DIRECTIONS, FOR THE 100 EXPERIMENTS USING THE PROPOSED METHOD AND THE ONE REPORTED IN [9].

Target No.	1	2	3	4	5
North Position (m)	15.49	10.73	24.83	24.46	15.26
North Position (m)[9]	11.78	12.54	26.32	31.9	23.12
East Position (m)	13.58	6.08	14.28	8.71	7.6
East Position (m)[9]	9.69	10.28	16.38	13.07	11.41

The technique is used to geo-localize and track multiple mobile targets using a dynamic weighted graph to determine regions with a high target density. A Model Predictive Control technique is used to optimize the camera pose which minimizes the overall uncertainty of target locations. The numerical results of the proposed algorithm show that the overall estimation errors improved when compared to the

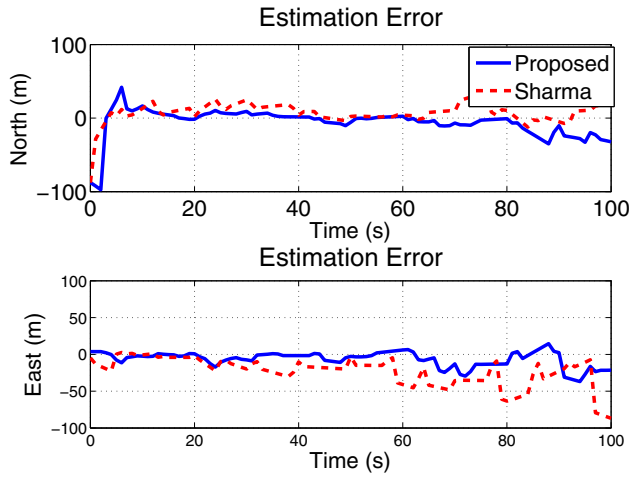


Fig. 7. Geo-location errors resulted from running the proposed method and the one reported in [9] for Target 2.

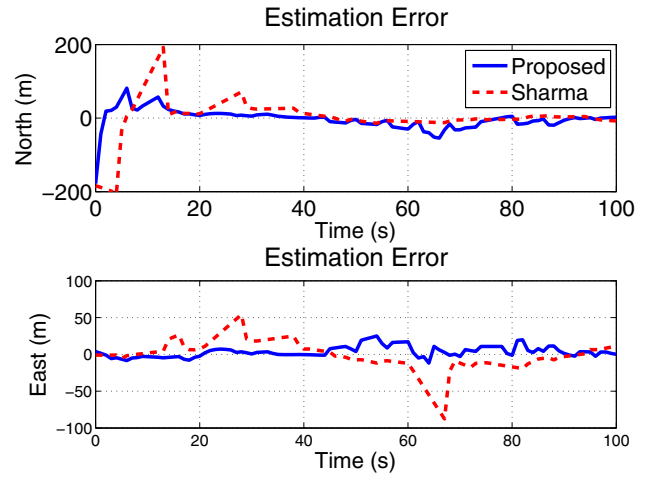


Fig. 9. Geo-location errors resulted from running the proposed method and the one reported in [9] for Target 4.

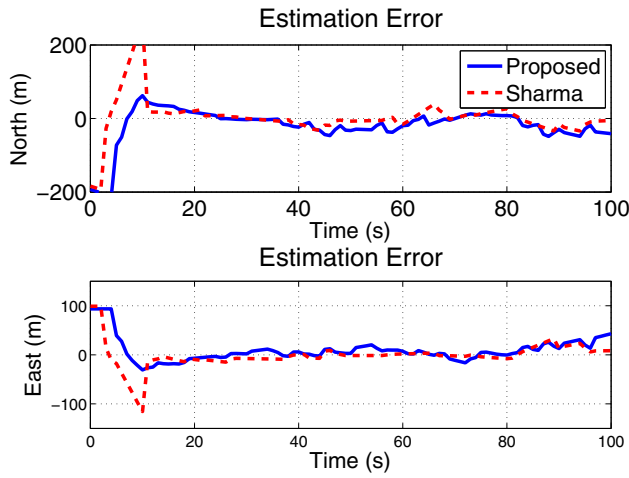


Fig. 8. Geo-location errors resulted from running the proposed method and the one reported in [9] for Target 3.

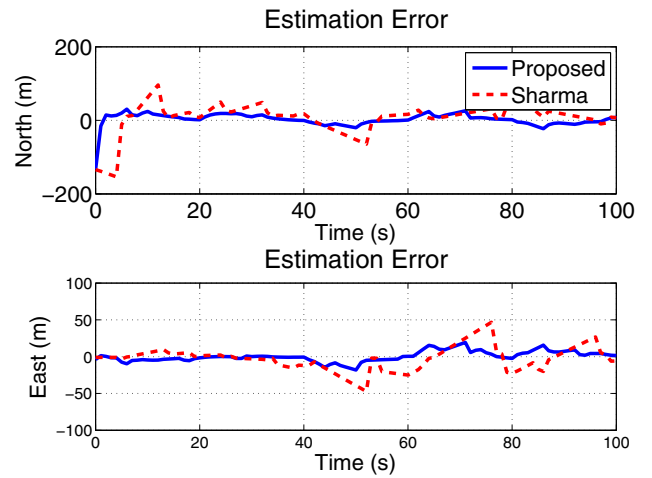


Fig. 10. Geo-location errors resulted from running the proposed method and the one reported in [9] for Target 5.

TABLE II

OVERALL AVERAGE OF GEO-LOCATION ERRORS IN EAST AND NORTH DIRECTIONS

Overall Error	Error	Difference (%)
Overall Error in North Position (m)	18.15	14
Overall Error in North Position (m)[9]	21.14	
Overall Error in East Position (m)	9.94	16
Overall Error east Position (m)[9]	11.91	

ones we previously reported. We plan to extend the current work to the task of multiple UAVs cooperatively tracking multiple targets

#### ACKNOWLEDGMENT

The authors acknowledge the contribution of Dr.Rajnikant Sharma for his help in providing the original simulation software.

#### REFERENCES

- [1] J. D. Redding, T. W. McLain, R. W. Beard, and C. N. Taylor, "Vision-based target localization from a fixed-wing miniature air vehicle," in Proc. American Control Conference, Minneapolis, MN, June 2006, pp. 2862-2867.
- [2] P. Theodorakopoulos and S. Lacroix, "UAV target tracking using an adversarial iterative prediction," in Proc. International Conference on Robotic and Automation, Kobe, Japan, 2009, pp. 2866-2871.
- [3] Z. Li, N. Hovakimyan, V. Dobrokhodov, and I. Kaminer, "Vision-based target tracking and motion estimation using a small UAV," in Proc. 49th IEEE Conf. Decision and Control (CDC), Atlanta, GA, December 2010, pp. 2505-2510.
- [4] K. Han and G. N. DeSouza, "Multiple targets geolocation using SIFT and stereo vision on airborne video sequences," in Proc. International Conf. Intelligent Robots and Systems (IROS), St. Louis, October 2009, pp. 5327-5332.
- [5] B. Grocholsky, M. Dille, and S. Nuske, "Efficient target geolocation by highly uncertain small air vehicles," in Proc. International Conf. Intelligent Robots and Systems (IROS), San Francisco, CA, 2011, pp. 4947-4952.
- [6] J. Tisdale, A. Ryan, Z. Kim, D. Tornqvist, and J. K. Hedrick, "A multiple UAV system for vision-based search and localization," in



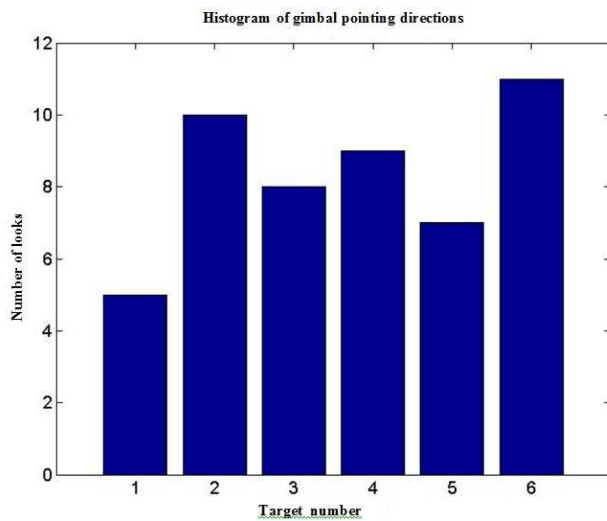


Fig. 11. Histogram of gimbal poses.

- Proc. American Control Conference, Seattle, WA, June 2008, pp. 1985-1990.
- [7] F. Morbidi and G. L. Mariottini, "Active Target Tracking and Cooperative Localization for Teams of Aerial Vehicles," *IEEE Trans. Control System Technology*, vol. 21, no. 5, pp. 1985-1990, September 2013.
  - [8] M. Ahmed and K. Subbarao, "Estimation based cooperative guidance controller for 3D target tracking with multiple UAVs," in Proc. American Control Conference (ACC), Montreal, Canada, June 2012, pp. 6035-6040.
  - [9] R. Sharma and D. Pack, "Cooperative Sensor Resource Management for Multi Target Geo-localization using Small Fixed-wing Unmanned Aerial Vehicles," in Proc. AIAA Guidance, Navigation, and Control (GNC) Conference, American Institute of Aeronautics and Astronautics, 2013.
  - [10] S. Thrun, Y. Liu, D. Koller, A. Y. Ng, Z. Ghahramani, and H. Durrant-Whyte, "Simultaneous localization and mapping with sparse extended information filters," *The International Journal of Robotics Research*, vol. 23, no. 78, pp. 693-716, 2004.
  - [11] Beard, Randal W., and Timothy W. McLain. *Small Unmanned Aircraft: Theory and Practice*, Princeton University Press, 2012.